www.czasopisma.pan.pl PAN POLSKA AKADEMIA NAUK www.journals.pan.pl

Arch. Metall. Mater. **65** (2020), 1, 375-384

DOI: 10.24425/amm.2020.131740

J. KAMIŃSKI[1*], K. MAŁKIEWICZ[2], J. RĘBIŚ[1], T. WIERZCHOŃ[1]

THE EFFECT OF GLOW DISCHARGE NITRIDING ON THE CORROSION RESISTANCE OF STAINLESS STEEL ORTHODONTIC ARCHES IN ARTIFICIAL SALIVA SOLUTION

The oral cavity due to its temperature fluctuations, changing pH, high humidity, action of mechanical forces and the presence of microorganisms is a favorable environment for degradation of dental materials. The paper presents comparative results on orthodontic arch-wires AISI304 steel before and after low temperature plasma nitriding carried out at cathodic potential (conventional) and at plasma potential, i.e. in a process incorporating an active screen. Corrosion resistance test on nitrided layers produced on stainless steel were carried out via electrochemical impedance spectroscopy (EIS) and the potentiodynamic method in non-deaerated artificial saliva solution at 37°C. The results were complemented with analysis of the structure, surface topography and microhardness. The results showed an increase in corrosion resistance of AISI304 steel after conventional glow-discharge nitriding.

Keywords: steel orthodontic arch-wires, artificial saliva, glow-discharge nitriding, corrosion resistance

1. Introduction

Metal alloys which are used for production of components of fixed orthodontic appliances undergo continuous degradation in the oral environment due to corrosive processes taking place there. Metal ions released into the body may have cytotoxic, mutagenic or carcinogenic properties as well as they can cause allergic reactions. Particularly noteworthy are nickel ions, whose participation in induction of hypersensitivity reactions is widely documented in the world literature [1,2]. The main material used in production of orthodontic arch-wires is austenitic alloy steel grade X5CrNi18-10 (AISI304) containing about 18% chromium and 8% nickel. During the time metal alloys are exposed to high humidity, temperature fluctuations, changing pH, mechanical stressing and the presence of microorganisms [3], degradation of orthodontic wires made of stainless steel can occur [4]. Due to corrosion of wires, the oral environment can be invaded not only by nickel ions but also by chromium [5], which is classified as a factor inducing development of cancer according to the International Agency for Research on Cancer [6].

The corrosion of fixed orthodontic braces is of interest to both clinicians and researchers dealing with the issue of biocompatibility of medical materials. In order to increase the biocompatibility various methods or/and surface engineering treatments of orthodontic arches are used. Manufacturers modify the surface of alloys with nitrogen or gold ions, metal oxides or polymeric materials [7-9]. This technique evokes high hopes in the context of increasing corrosion resistance of medical materials and improvement of surfaces' mechanical properties. One of the methods used to implement nitrogen on the surface of metal alloys is the glow discharge nitriding process [10,11]. Due to constant development of metallurgical techniques and increased demands regarding construction materials, it has been significantly modified as a result of its combination with other glow treatment techniques (e.g. CVD, PVD) or the combination of glow discharge nitriding with oxidation (the process of oxynitriding) [12-17]. All these modifications allow full control of the distribution and thickness of the obtained layers, as well as creation of modern composite and multi-component layers, characterized by high resistance to wear caused by friction, increased corrosion resistance, or increased resistance to oxidation at higher temperatures. By controlling the parameters of the processes carried out under glow discharge conditions, namely temperature, time, composition of the gas mixture and pressure in the working chamber, layers can be produced which have controlled chemical and phase composition, microstructure and surface topography [7,10-17].

The aim of the study was to determine the impact of a nitrided layer produced under glow discharge condition, conducted

[1] WARSAW UNIVERSITY OF TECHNOLOGY, FACULTY OF MATERIALS SCIENCE AND ENGINEERING,141 WOLOSKA STR., 02-507 WARSZAWA, POLAND
[2] MEDICAL UNIVERSITY OF LODZ, DEPARTMENT OF ORTHODONTIC, 4 TADEUSZA KOŚCIUSZKI AV., 90-419 LODZ, POLAND

* Corresponding author: jmkaminsk@gmail.com

under cathode (CP) [15] and plasma potentials (PP) [18], on steel orthodontic arches on their corrosion resistance in artificial saliva solution.

2. Materials and methods

The materials of the research were edge arches of the 0.017 × 0.025 inch (0.04 × 0.06 cm) size made of the stainless steel type AISI 304, provided by two different producers: Dentaurum (Germany) and Centraliss (China). The surface of all of the wires had been pre-treated by the manufacturer. Surface finishing state (e.g. roughness) of the examined wires varied (Tab. 3). Technology used to obtain it is most of the time producer's secret due to unique interrelation of technology used and wires mechanical properties, so much desired in the process of orthodontic treatment. From the orthodontic wires described above, six arches specimens ((2 x initial state (IS), 2 x plasma potential (PP) and 2 x cathode potential (CP)) of 2 cm length were prepared, five for each type of arch. The surface area of each tested material was 0.4 cm^2. The chemical composition of the tested materials is presented in Table 1 (determined by EDS – Energy Dispersive Spectroscopy).

TABLE 1

AISI304 chemical composition (wt. %) (determined by EDS)

	Cr	Ni	Mn	Al	Mo	Cu	Si	Fe
Dentaurum	19.0	8.5	1.5	0.2			0.6	rest
Centraliss	19.0	7.2	1.0	0.1	0.2	1.0	0.4	rest

Glow-discharge nitriding processes of steels samples were carried out at the following process parameters: temperature 330°C, under pressure in the reaction chamber of 150 Pa in an atmosphere of gaseous mixture hydrogen and nitrogen (3/1) for 6 h. Immediately before nitriding, the samples were subjected to cathodic sputtering in pure hydrogen at a pressure of 30 Pa for 15 min. This process allowed both for surface cleaning and activation of the surface of the treated steel. The processes were carried out via conventional glow-discharge nitriding at cathodic potential (CP) and using an active screen (PP). The following electrical paremeters of glow-discharge treatment were applied: at CP – 520V; 0.95A and at PP – 510V; 1.45A.

The surface topography of the nitrided layers was measured by means of a WYKO NT 9300 scanning optical profilometer, the microhardness (HV0.02) using a Zwick Materialprufung 3212002 microhardness meter. The microstructure of the produced layers was studied by preparing metallographic sections via grinding by means of 600-2500 grit sandpapers, followed by polishing in a SiO_2 silicon dioxide suspension. Surfaces prepared this way were then electrochemical etched in 10% oxalic acid (3V, dc, 5s). Longitudinal observations were carried out using a Nikon Eclipse LV150N light microscope. The initial surface and nitrided layers were observed using the Scanning Electron Microscope (SEM) HITACHI SU 90 equipped with an adapters for microanalysis in microareas (EDS – Energy Dispersive Spectroscopy and WDS – Wave Dispersive Spectroscopy) produced by Thermo Noran. Nitrided layers were observed in secondary electron (SE) mode on the surface – longitudinal – (before) and in cross-section (transversal) after electrochemical etched. The phase composition was examined in a Brucker D8 Discover X-ray diffractometer in a Bragg-Brentano geometry using Cu Kα (λ = 0.154056 nm) radiation at room temperature. The recording conditions of the XRD spectrum were as follows: voltage 40 kV, current 40 mA, angular range 2Θ from 25° to 60°, step Δ2Θ – 0.05°, counting time – 3 s. The XRD spectrum were analysed using Brucker EVA software.

Electrochemical tests were performed in artificial saliva [19], whose composition is shown in Table 2.

TABLE 2

Chemical composition of artificial saliva solution [g dm^{-3}] (pH 5.7)

Compound	NaCl	KCl	NaH_2PO_4	$CO(NH_2)_2$	$CaCl_2 \times 2H_2O$	$Na_2S \times 9H_2O$
Quantity	0.4	0.4	0.69	1	0.906	0.005

Corrosion resistance examinations were carried out by means of the impedance and the potentiodynamic methods using an Autolab PGSTAT100 potentiostat/galwanostat (Eco Chemie B.V., Holand) with FRA2 module, in non-deaerated artificial saliva solution at 37 °C. Prior to electrochemical tests, the samples were exposed to the artificial saliva solution in current-free conditions for 120 min. Impedance examination was conducted in a three-electrode setup: the test electrode – reference electrode (saturated calomel electrode (SCE)) – auxiliary electrode (platinum), with the frequency ranging from 10^5 Hz to 10^{-3} Hz and use of AC signal with an amplitude of 5 mV. Corrosion cell was kept in a Faraday cage. EIS methods were recorded in the potentiostatic mode at open circuit potential (E_{OCP}). Eco Chemie Analyst software [EQUIVRT – Baukamp program] was used for processing and fitting the impedance spectra. An equivalent circuit (EC) with two time constants R(Q[R(RQ)]) (Fig. 1) was used, which is generally applied in the case of materials susceptible to local corrosion [20]. Obtained spectra were presented in the form of Bode plot. Potentiodynamic tests were conducted in an identical trielectrode setup, up to a potential of 1500 mV, or up to achieving currents over 1 mA/cm^{-2}. The test material was polarized with a potential sweep rate of 0.2 mV s^{-1}.

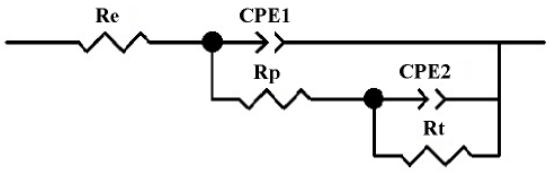

Fig. 1. Electric equivalent circuit (EC) with two time constant models R(Q[R(RQ)]) used for interpretation of the corrosion behaviour of AISI304 alloy in artificial saliva solution;
Re – environmental resistance, Rp – resistance of dielectric layer, Rt – charge transfer resistance through double layer, CPE1 – capacitance of constant phase element of passive layer, CPE2– capacitance of constant phase element of double layer

3. Results

Fig. 2 presents electrochemically etched (10% oxalic acid, 5V, dc, 5s) initial surface microstructure of examined materials.

Structural analysis of Dentaurum orthodontic wire (Fig. 2A) shows austenitic structure with chromium carbides ($Cr_{23}C_6$) [21] within. Minimum nickel concentration (8 Ni wt.%) which determines austenitic steel structure leads however to creating deformation martensite stripes during orthodontic wire drawing and can next lead to elongated cracks of the material. Additionally, bending stress developed in the process of arches forming is observed. In Centraliss orthodontic wire, structural analysis indicates presence of both chromium carbides ($Cr_{23}C_6$), and a two-phase austenitic-martensitic structure (Fig. 2B). Martensite phase is explained with decreased level of nickel (7.2 Ni wt.%) in orthodontic wire of Centraliss (Table 1). Decreased level of nickel enables deformation martensite phase development in bulk during orthodontic wires drawing. Copper presence (1.0 Cu wt.%) in Centraliss alloy has on one hand positive impact on its bacteriostatic and bactericidal parameters leading to reduced bacteria colonization in oral environment, but on the other hand multi-phase alloy can adversely affect corrosion resistance and longevity of orthodontic arch. In addition, in bending stress zone deformation martensite phase is observed.

Use of glow discharge nitriding allows forming of homogeneous structurally diffused nitrided layers on tested materials. Fig. 3 shows the microstructure of the nitrided layers produced.

In the case of the conventional nitriding process carried out on the Dentaurum wires, the thickness of the nitrided layer, so-called nitrogen austenite (Fig. 4, [22]) is about 2.5 μm, while wires with significant initial roughness (Centraliss), despite the use of identical technological parameters, demonstrate the thickness of the layer comparable to the data observed for the active screen use (about 1.5 μm). The chemical composition tests showed the presence of nitrogen in the layer produced in conventional processes, in amounts of approx. 7.3 N wt.% (Dentaurum) and 5.7 N wt.% (Centraliss), while the active screen (PP) use showed respectively 4.8 N wt.% and 3.8 N wt.%.

Fig. 4 presents the diffractogram of nitrided layers (S phase) [22] produced in conventional (CP) glow-discharge nitriding on Dentaurum and Centraliss orthodontic wires.

Nitrided layers produced on AISI 304 steel of austenic γ structure (Dentaurum), independent of glow-discharge nitriding technology used, show single-phase structure of nitrogen austenite γN, known also as S phase [22]. During nitriding at 330°C proces regular face-centered cubic structure (A1) austenite γ transforms into tetragonal structure austenite γN. Additionally, in initial material (Fig. 4A), apart from phase γ peaks, an extra peak of ca. $2\Theta = 44.5°$ angle is observed, which indicates body-centered cubic structure deforming martensite presence (A2), developed during technological wires drawing. In glow-discharge nitrogening process deforming martensite α' transforms into nitrogen martensite and next in nitrogen austenite γ, thus martensite α' cannot be seen in nitrogened layers any more [24]. In case of Centraliss wire (Fig. 4B), considerable part of deforming martensite, whose peak also fades away during glow-discharge treatment, is observed, apart from typical austenic phase, in XRD spectrum. It can be assumed that significant share of magnetic phase in orthodontic wire is caused by partial transformation of austenite into deforming martensite during orthodontic wires drawing. Decreased nickel concentration (7.3 Ni wt. %) in the alloy disabled proper austenite phase stabilizing during technological treatment. Phase composition of layers produced with active screen use is identical to layers produced in classic glow-discharge nitriding. Characteristic peaks intensity differences are caused by thinner nitride layers produced.

Fig. 5 presents diverse topographies of the layers depending on the technology used for their formation.

In the case of layers produced with use of active screen (PP) on Dentaurum arches, coat roughness of the surface layer is comparable to the steel surface in the initial state (IS) (Table 3). At the same time, layers produced in the classic glow nitriding process (Fig. 6, Table 3) show an increase in roughness of the layer, which is an effect of the cathode sputtering [18].

When steel surface showed higher roughness in the initial state (Centraliss), the cathodic sputtering process lead to smooth-

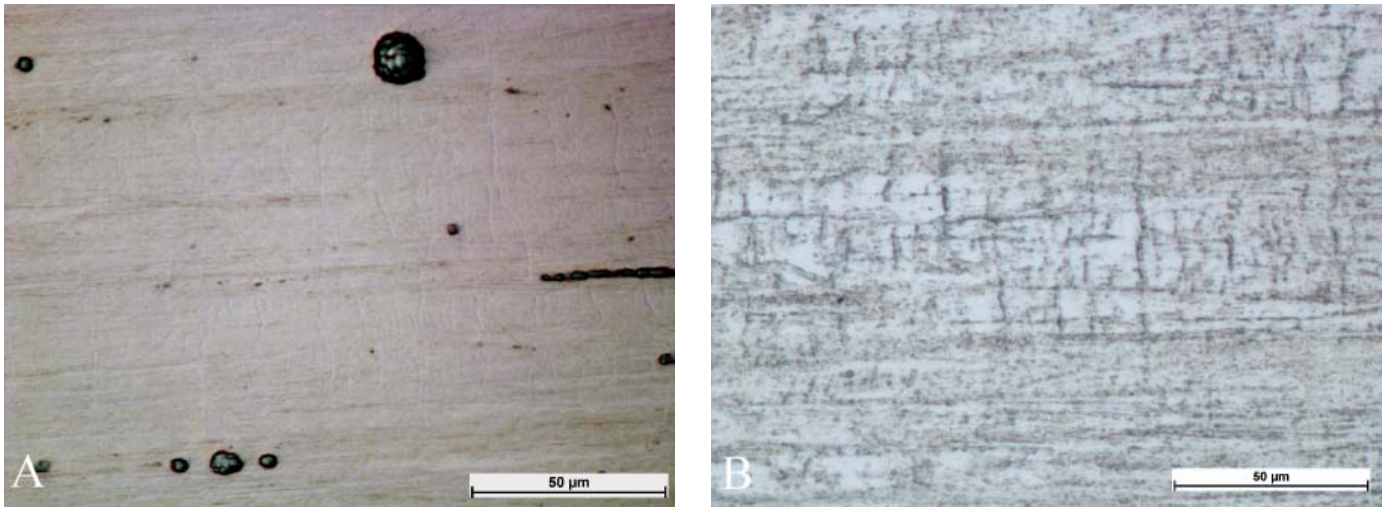

Fig. 2. Arch-wire microstructure initial state (electrochemically etched); A) – Dentaurum, B) – Centraliss (light microscope)

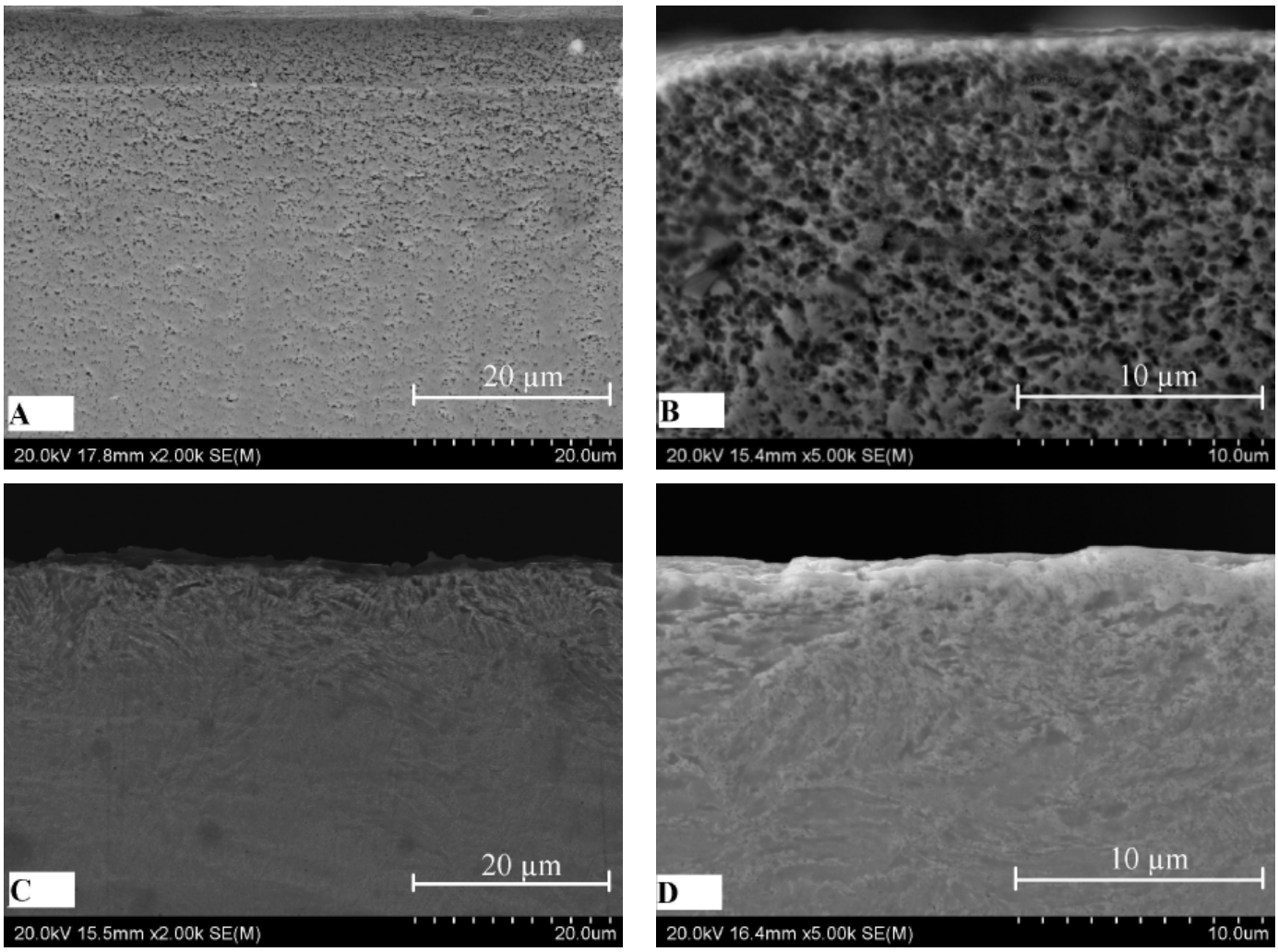

Fig. 3. Microstructures of nitrided layers produced on AISI304 steel on Dentaurum arches (A, B) and Centraliss arches (C, D) depending on the glow nitriding technology used. (A), (C) – CP; (B), (D) – PP

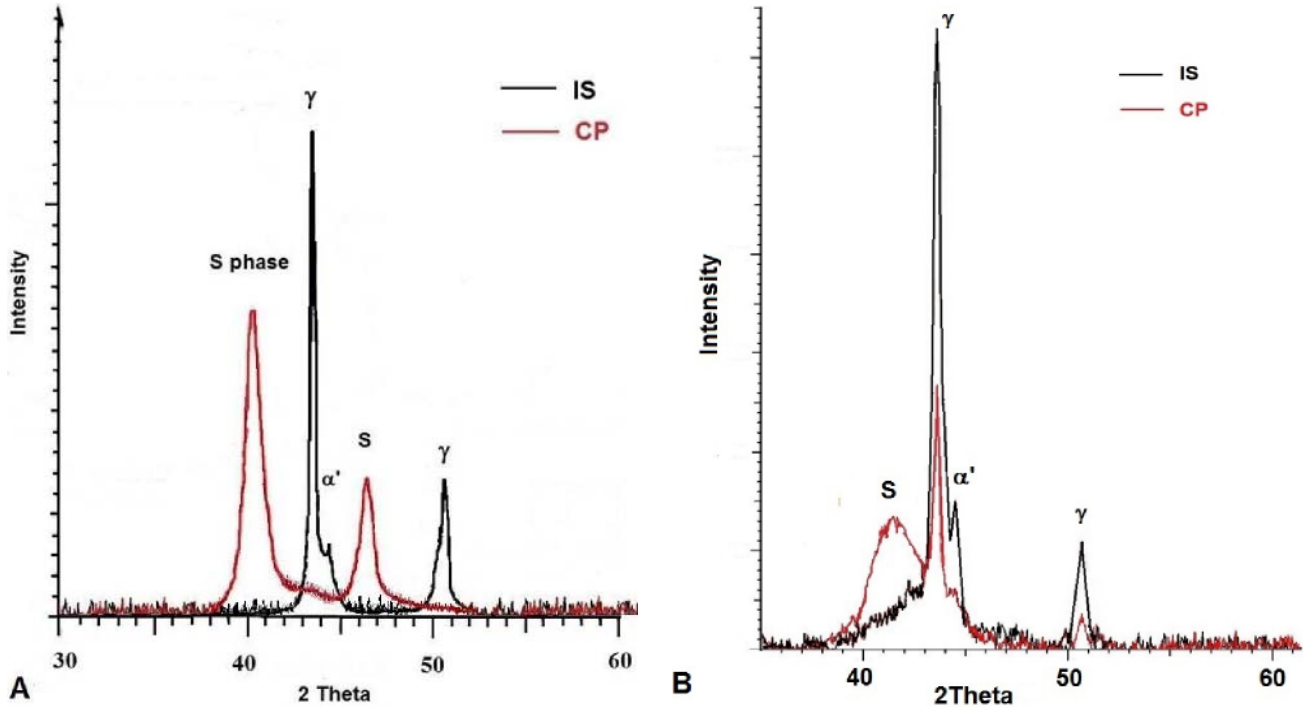

Fig. 4. Diffractogram of the nitrided layers (CP) produced on AISI304 steel under glow discharge conditions in comparison to starting material (IS).

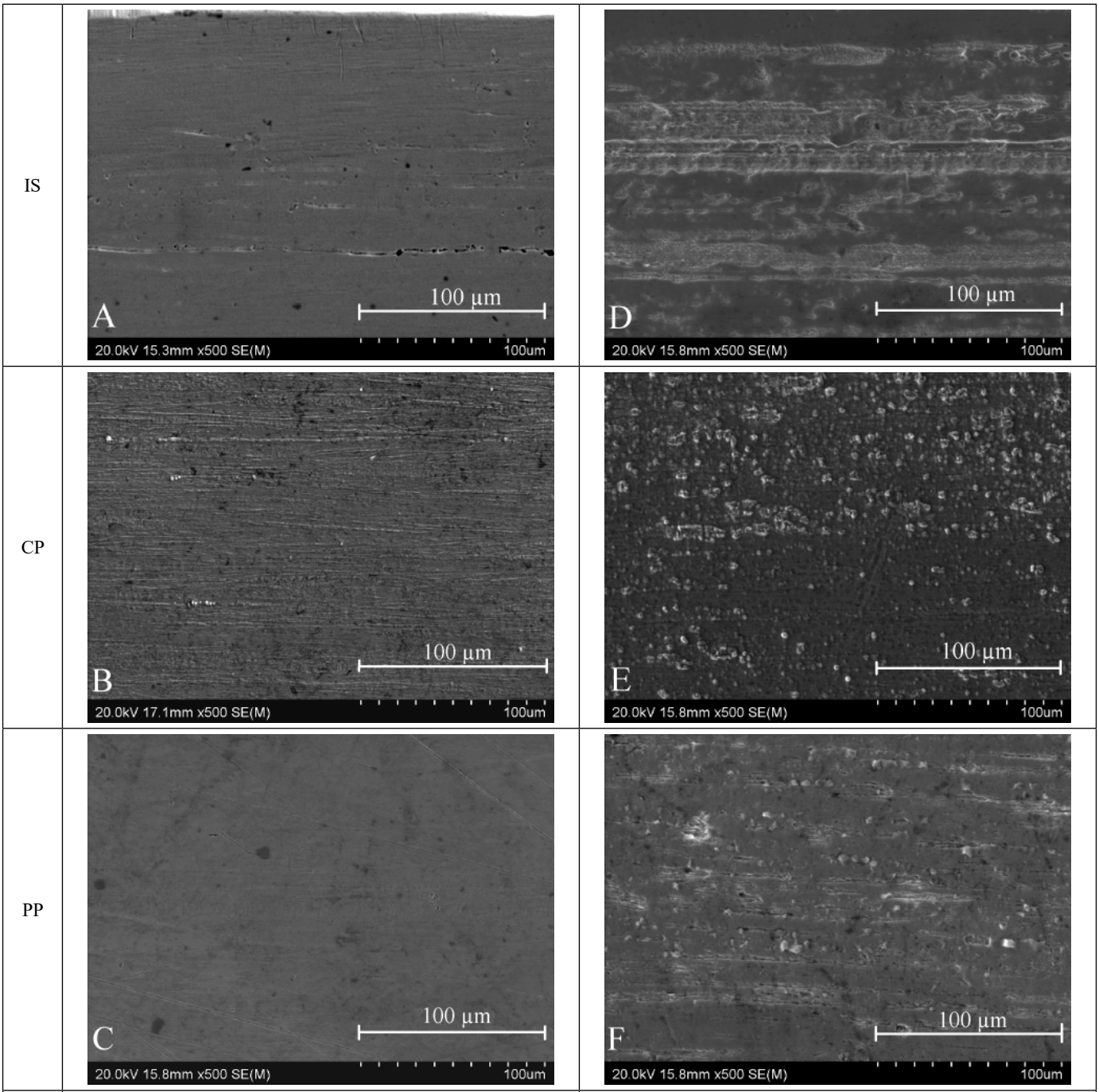

Fig. 5. Surface topography (SEM) of nitrided layers produced on AISI304 steel on Dentaurum (A, B, C) and Centraliss (D, E, F) arches, produced at the cathode (B, E) and plasma (C, F) potentials in comparison to initial material (A, D)

TABLE 3

Surface roughness parameters of nitrided layers in comparison to stainless steel in initial state [µm]

		Ra [µm]	SD	Rq [µm]	SD	Rz [µm]	SD	Rt [µm]	SD
Dentaurum	**IS**	**0.026**	0.002	**0.033**	0.003	**0.634**	0.034	**1.088**	0.132
	CP	**0.085**	0.003	**0.119**	0.004	**2.196**	0.124	**2.893**	0.130
	PP	**0.035**	0.003	**0.049**	0.006	**1.600**	0.080	**2.220**	0.386
Centraliss	**IS**	**0.992**	0.154	**1.230**	0.169	**13.087**	0.786	**15.897**	1.114
	CP	**0.672**	0.028	**0.907**	0.052	**16.842**	0.897	**19.412**	1.719
	PP	**0.726**	0.035	**0.968**	0.052	**15.118**	1.199	**18.792**	2.912

Ra – average arithmetic deviation of the roughness profile from the median line; **Rq** – average square of the roughness profile from the median line along the measurement of elementary length; **Rz** – distance from the highest point of the roughness profile to its lowest point measured along the elementary length; **Rt** – distance from the highest point of the roughness to its lowest point; **SD**-standard deviation

ing of the surface (Table 3), which, among others, effects on corrosion resistance [9] and biological properties [23]. Fig. 6 shows changes in surface topography, depending on the glow treatment applied, in comparison to the starting material.

Cathode sputtering is of higher impact at the edges of orthodontic wires and its effects can be especially noticed in the wires of low roughness in the initial state (Dentaurum) (Fig. 7). This is so-called edge effect within which more intense phenomena accompanying sputtering such as increase in the thickness of nitrided layer, nitrogen concentration in the layer or the possibility of local formation of chromium nitrides occur (CrN) [13]. In the case of layers generated at the plasma potential, differences in microhardness within the sample are significantly smaller. Fig. 7 presents the microhardness distribution in the tested materials.

The increase in microhardness of the tested materials is related to the formation of nitrogen austenite (S phase) [13]. Due to relatively low temperature of the process, no CrN phase was detected (Fig. 4). Microhardness increase at the edges of the arcs (up to 1200 HV0.02) is caused by higher nitrogen level in surface layer.

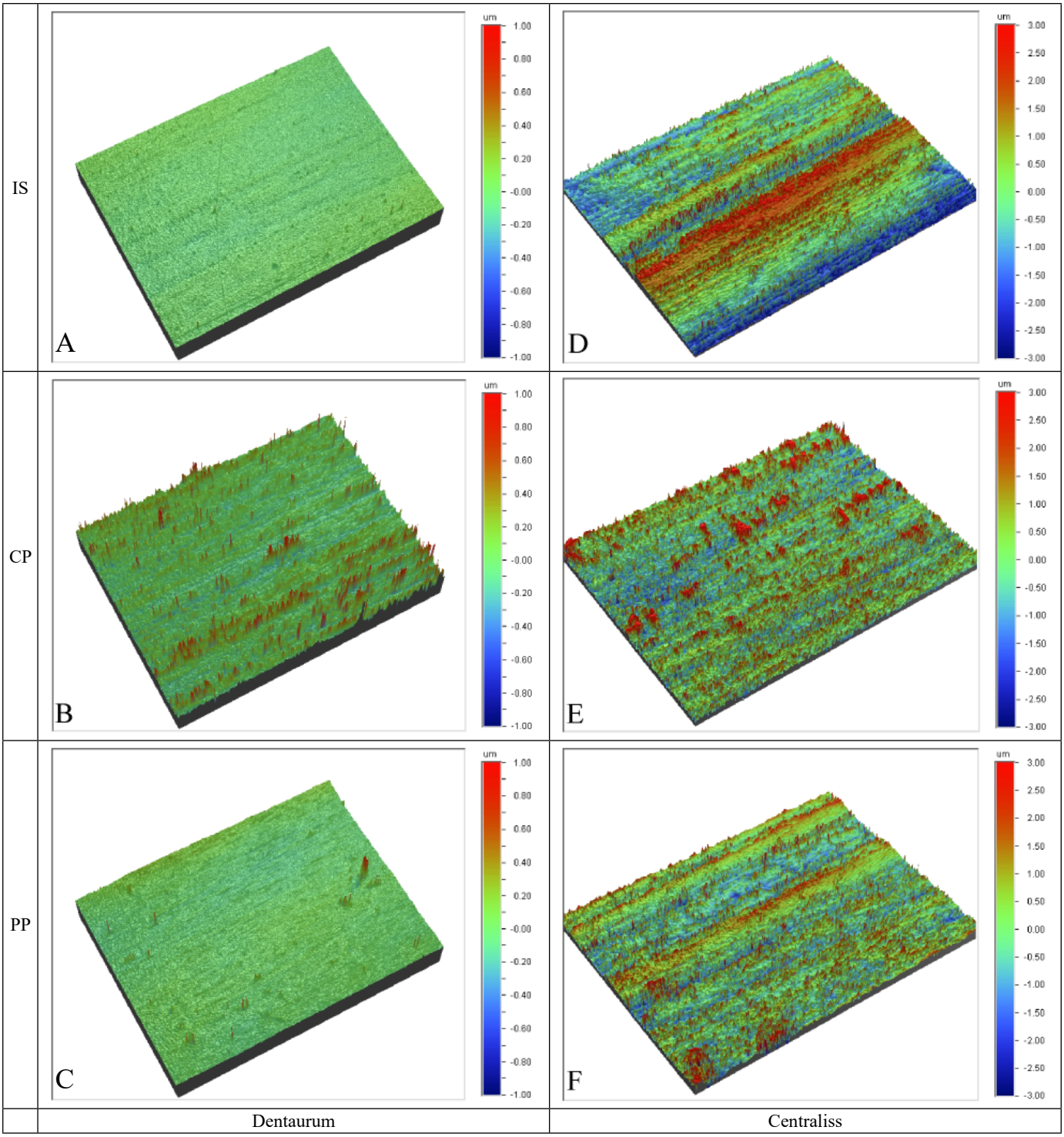

Fig. 6. Surface topography (optical profilometer) of nitrided layers produced on AISI304 steel on Dentaurum (A,B,C) and Centraliss (D,E,F) arches produced at the cathode (CP)(B,E) and plasma (PP) potentials (C,F) compared to the initial state (IS) (A,D)

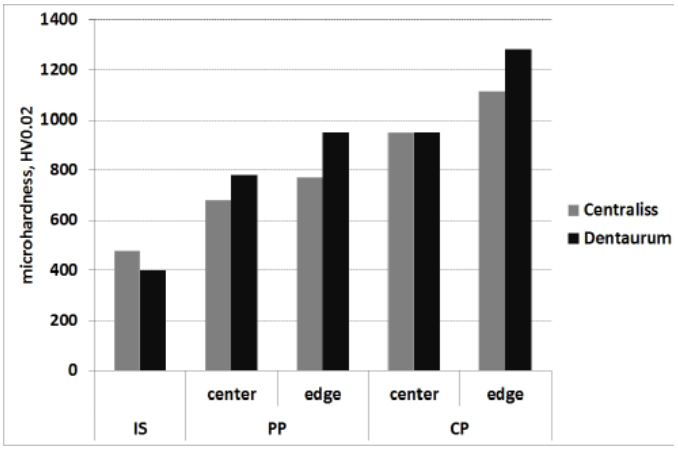

Rys. 7. Microhardness of nitrided layers (PP or CP) compared to untreated material (IS)

Due to chromium nitride (CrN) absence and low concentration of chloride ions in the artificial saliva solution (0.8708 g dm^{-3} Cl^-) pitting corrosion was not observed in a wide range of potentials tested (Fig. 9 and Fig. 10). In the case of nitrided layers with greater roughness (Centraliss wires) pitting corrosion was found in the range of higher potentials, regardless of the technology of glow discharge nitriding used (i.e. PP or CP). The pitting corrosion initiator is here the heterogeneous structure of the surface layer; however increased internal stresses in the layer can be a corrosion trigger too.

Fig. 8 shows the impedance spectra (Bode plots) of nitrided layers produced at the cathode (CP) and plasma (PP) potentials on Dentaurum and Centraliss orthodontic wires while Table 4 presents the characteristic electrochemical values of the materials studied.

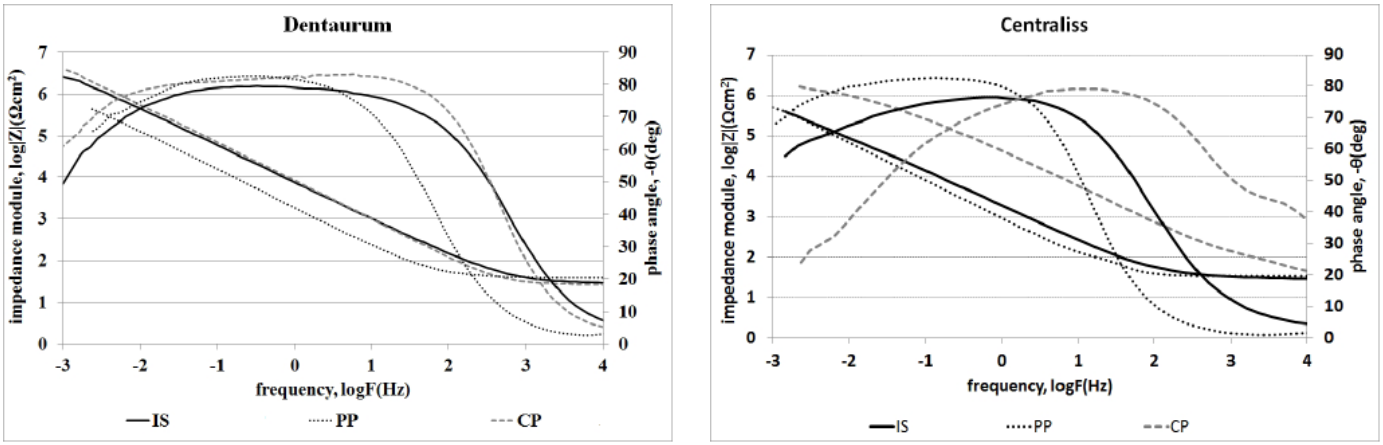

Rys. 8. Bode plots of nitrided layers formed at plasma potential (PP) and cathodic potential (CP) compared to untreated materials [IS]

TABLE 4

Characteristic electrochemical values of examined orthodontic arches (impedance tests)

			Solution	Dielectric layer		Electric double layer
Dentaurum	IS	R (Ωcm^2)	29	5.49×10^2		4.43×10^6
		Y_{oCPE} ($Fcm^{-2}s^{n-1}$)		2.03×10^{-5}		5.05×10^{-6}
		n		0.869		0.863
	CP	R (Ωcm^2)	26	3.09×10^5		9.58×10^6
		Y_{oCPE} ($Fcm^{-2}s^{n-1}$)		2.09×10^{-5}		2.02×10^{-6}
		n		0.932		0.756
	PP	R (Ωcm^2)	30	3.09×10^3		4.58×10^5
		Y_{oCPE} ($Fcm^{-2}s^{n-1}$)		2.09×10^{-3}		2.02×10^{-4}
		n		0.98		0.89
Centraliss	IS	R (Ωcm^2)	34	5.32×10^5		4.79×10^5
		Y_{oCPE} ($Fcm^{-2}s^{n-1}$)		1.10×10^{-5}		1.50×10^{-4}
		n		0.85		1
	CP	R (Ωcm^2)	26	76	2.96×10^4	2.69×10^6
		Y_{oCPE} ($Fcm^{-2}s^{n-1}$)		7.2×10^{-6}	3.7×10^{-6}	1.9×10^{-6}
		n		0.78	0.918	0.5
	PP	R (Ωcm^2)	36	2.80×10^4		7.82×10^5
		Y_{oCPE} ($Fcm^{-2}s^{n-1}$)		1.63×10^{-4}		1.25×10^{-4}
		n		0.82		0.97

R – resistance, Yo_{CPE} – capacity of constant phase element, n – coefficient of imperfections of constant phase element (CPE); an empirical constant ranging from 0 to 1. It is worth noting that when n = 1, the CPE behaves as a pure capacitor, while when n = 0, the CPE behaves as a pure resistor.

Bode's plots (Fig. 8) analysis indicates the presence of at least two time constants in all examined cases, demonstrating two electrochemical processes taking place on the tested surfaces. Equivalent circuit R(Q[R(RQ)]) (Fig. 1) was used to analyse plots. For the initial material of Dentaurum wire it can be assumed that the analyzed peaks describe electrochemical parameters occurring on smoother surfaces observed on the inner surface and near the edges of the arches characterized by increased roughness (Fig. 5). Differences observed in surface topography of the analyzed areas may result from the location of internal stresses accompanying the process of wire drawing and strain hardening. In the case of Centraliss wires, the observed peaks describe electrochemically polished areas adjacent to etched areas (in the form of gully) with high roughness. Significant development of the wires surface (Fig. 5) indicates that the process of electrochemical polishing was not fully refined.

For nitrided layers of Dentaurum wire, which were produced at the cathode potential, an increase in electrochemical inhomogeneity of materials is observed, manifested by clearly marked two maxima of phase angles in Bode's plots. This result points to the topography of the surface layer and in particular the processes accompanying the edge effect as the factors determining the shape of the spectrum. Only in the case of materials with a higher initial roughness (Centraliss) the observed edge effect and processes accompanying sputtering do not cause a significant differentiation of the surface topography (Ra parameter decreases from 0.98 µm (IS) to 0.8 µm (CP) and 0.9 µm (PP)), but only an increase in the electrochemical heterogeneity of the surface layer. The roughness parameters, and in particular the Rt parameter (determining space between lowest and highest points) which increase from 15.8 µm (IS) to 19.4 µm (CP), indicate surface development. The high roughness parameters (Table 3) and the results of impedance tests (Table 4) show the decisive influence of diffusion (n = 0.5) on the electrochemical parameters of the layer.

In the case of plasma nitrided layers, due to the technological parameters used, the layers formed are thinner (about 1.5 µm), hence of lower hardness (650 – 800 HV0.02) but with a roughness similar to the initial material (Fig. 5). For substrates of lower roughness (Dentaurum), the presence of a homogeneous layer of nitrided austenite translates into resistance to pitting corrosion in a wide range of potentials tested. The observed increase in the current density (at approx. 1000 mV) is associated with oxygen liberating from the solution. Substrates of higher roughness demonstrate heterogeneous and discontinuous nitrided austenite layer (Fig. 5F), which negatively affects resistance of steel to pitting corrosion. At the same time, the values of the impedance modules, defining the Faraday current values, indicate a different corrosion resistance of the tested layers: nitrided layers produced on Centraliss wires increase the corrosion resistance of orthodontic wires; this effect was not achieved on homogenous layers produced on orthodontic wires of Dentaurum.

Fig. 10 shows surface topographies after potentiodynamic examinations. Dentaurum wires show pitting corrosion in initial state. In case of nitrided layers produced with use of active screen

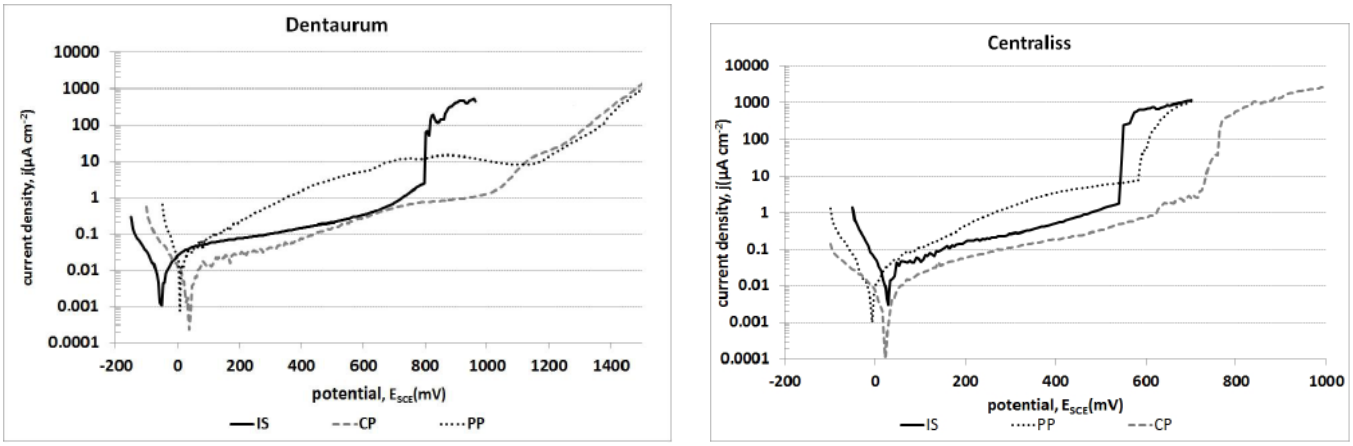

Fig. 9. Potentiodynamic curves of nitrided layers produced on AISI 304 stainless steel orthodontic wires by Dentaurum and Centraliss, exposed to artificial saliva solution at 37°C

TABLE 5

Characteristic electrochemical values of examined orthodontic arches (potentiodynamic tests)

		No. of samples	I_{corr} [µA cm^{-2}]	Median	Std dev	E_{corr} [mV $_{SCE}$]	E_{np} [mV $_{SCE}$]
Dentaurum	**IS**	5	0.009	0.010	0.003	–55	770
	PP	5	0.028	0.028	0.008	10	—
	CP	5	0.003	0.002	0.003	35	—
Centraliss	**IS**	5	0.030	0.029	0.007	40	530
	PP	5	0.011	0.009	0.005	–10	580
	CP	5	0.004	0.006	0.003	25	710

E_{corr} – corrosion potential, I_{corr} – corrosion current density, E_{np} – pitting potential.

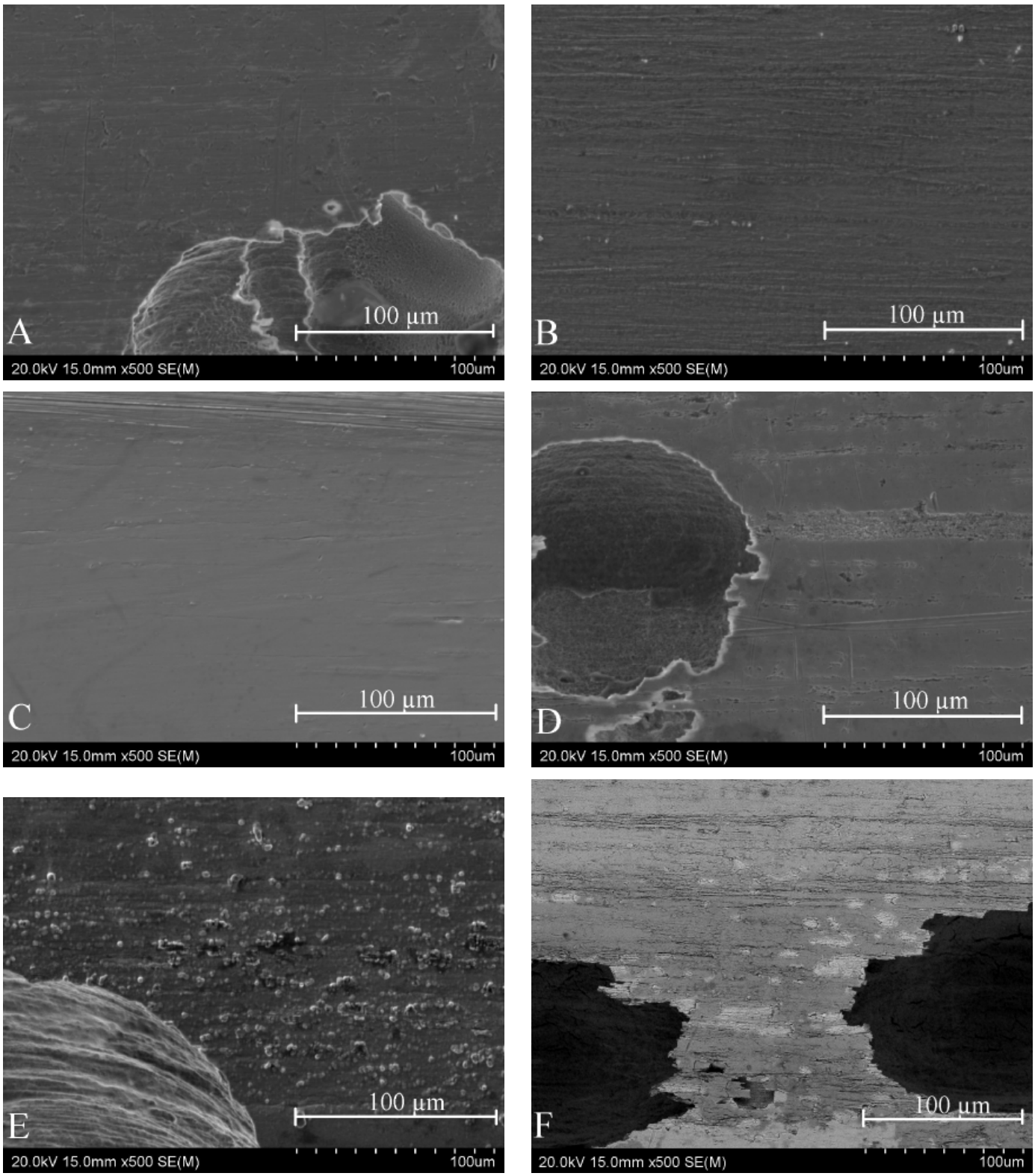

Fig. 10. Surface topography (SEM) after potentiodynamic tests in artificial saliva at 37°C of nitrided layers produced on AISI304 steel on Dentaurum (A, B, C) and Centraliss (D, E, F) arches, produced at the cathode (B, E) and plasma (C, F) potentials in comparison to starting material (A, D)

(PP) on Dentaurum wires, etching of cracks already noticed in initial state is observed. Classic nitrided layers (CP) produced on Dentaurum wires are not susceptible to corrosion in artificial saliva solution. Centraliss wires, irrespective of nitriding technology applied, demonstrate pitting corrosion (CP) or pitting and etching (PP) of layers.

4. Discussion and conclusions

Technology of the glow discharge nitriding is used to refine the surface of materials (NiTi, TMA) used in different branches of dentistry [25], i.e. endodontics, orthodontics, prosthetics and surgery. The goals of modifying dental materials are to improve

their biocompatibility, increase resistance to corrosion, reduce susceptibility to chemical agents and modify their physical properties, such as elasticity. Implanting orthodontic arches with nitrogen ions reduces irregularity of their surface as well as their friction [26], which can potentially contribute to shortening of orthodontic treatment time.

Available literature does not include information on resistance to corrosion of stainless steel orthodontic arches with modified glow discharge nitriding surface. Variable nickel concentration (8-10 Ni wt. %) translates into variable initial corrosion resistance of steel orthodontic wires and thus to variable corrosion resistance of nitrided layers produced on them. In materials of lower nickel concentration (<8 Ni wt. %) gradient increase of martensite stripes during wires drawing is observed, proportionally to decreasing nickel concentration. This extra phase is however not observed in case of alloys with nickel concentration >8 Ni wt. %. Finishing technology (e.g. recovery) also significantly impacts durability of passive nitrided layers [19]. Yet, simple correlation between corrosion resistance and singular parameter (e.g. rougness, chemical and phase composition) of surface layer was not observed in the cases analyzed. It can be only stated that classic nitriding process (CP), reducing the current density of stainless steel alloys about 5 times, may positively affect biological properties of materials used during orthodontic treatment, significantly increasing safety of their use. Of course, this technique requires further evaluation, in the context of impact on physical properties of steel arches such as hardness, flexibility or elasticity, which are conditioning their clinical usefulness.

1. The nitrided layers produced under glow discharge conditions on orthodontic wires increase both the corrosion resistance of the material and the durability of the passive layers formed. Use of the sputtering process significantly modifies surface topography of the substrate. In the case of substrates with low roughness, the surface develops (Ra increases from 0.026 μm to 0.085 μm), yet no adverse effect is observed on the formation of nitrided austenite layers with high resistance to electrochemical and pitting corrosions, due to use of low-temperature glow nitriding process. At the same time, cathode sputtering onto substrates with increased roughness results in lowering nano-roughness indices (Ra decreasing from 0.992 μm to 0.713 μm) while the distance between the highest and lowest measuring points (Rt increases from 15.8 μm to 19.4 μm) increases. This leads to increased resistance of formed nitrided austenite layer to electrochemical corrosion, but does not fully protect from local corrosion.
2. Due to the cathode sputtering phenomenon in glow discharge nitriding at low process temperatures and its beneficial effect on the formation of nitrogen austenite surface layers, a process of classical glow-discharge nitriding, i.e. at cathode potential, is a more prospective modification of orthodontic wires made of AISI304 steel.

REFERENCES

[1] J.C. Wataha, J.L. Drury, W.O. Chung, Expert Rev. Med. Devices. **10** (4), 519-539 (2013).
[2] T.P. Chaturvedi, S.N. Upadhayay, Indian J. Dent. Res. **21** (2), 275-284 (2010).
[3] M. Jaishankar, T. Tseten, N. Anbalagan, B.B. Mathew, K.N. Beeregowda, Interdiscip. Toxicol. **7** (2), 60-72 (2014).
[4] S.M. Castro, M.J. Ponces, J.D. Lopes, M. Vasconcelos, M.C.F. Pollmann, J. Dent. Sci. **10** (1), 1-7 (2015).
[5] D.M. Proctor, M. Suh, S.L. Campleman, C.M.Thompson, Toxicology **325**, 160-179 (2014).
[6] J. Palus, K. Rydzynski, E. Dziubaltowska, K. Wyszynska, A.T. Natarajan, R. Nilsson, Mutat. Res-Gen. Tox. En. **540** (1), 19-28 (2003).
[7] H. Zhang, S. Guo, D. Wang, T. Zhou, L. Wang, J. Ma, Angle Orthod. **86** (5), 782-788 (2016).
[8] V. Katić, H.O. Ćurković, D. Semenski, G. Baršić, K. Marušić, S. Špalj, Angle Orthod. **84** (6), 1041-1048 (2014).
[9] H. Sugisawa, H. Kitaura, K. Ueda, K. Kimura, M. Ishida, Y. Ochi, A. Kishikawa, S. Ogawa, T. Takano-Yamamoto, Dent. Mater. J. **37** (2), 286-292 (2018).
[10] E. Czarnowska, T. Wierzchon, A. Maranda-Niedbała, E. Karczmarewicz, J. Mater. Sci. Mater. Med. **11** (2), 73-81 (2000).
[11] J. Flis, Surf. Eng. **26** (1-2), 103-113 (2010).
[12] T. Wierzchon, E. Czarnowska, J. Grzonka, A. Sowinska, M. Tarnowski, J. Kaminski, K. Kulikowski, T. Borowski, K.J. Kurzydłowski, Appl. Surf. Sci. **334**, 74-79 (2015).
[13] S.C. Gallo, H. Dong, Surf. Coat. Techn. **203** (24), 3669-3675 (2009).
[14] E. Skolek, J. Kaminski, J. Sobczak, T. Wierzchon, Vacuum **85** (2), 164 -169 (2010).
[15] R.R.M. de Sousa, F.O. de Araujo, K.J.B. Ribeiro, M.W.D. Mendes, J.A.P. de Costa, C. Alves, Mater. Sci. Eng. **465** (1-2), 223-227 (2007).
[16] Y. Li, Y. He, S. Zhang, X. He, W. Wang, B. Hu, Vacuum, **146** (12), 1-7 (2017).
[17] A. Sowinska, E. Czarnowska, M. Tarnowski, J. Witkowska, T. Wierzchon, Appl. Surf. Sci. **436**, 382-390 (2018).
[18] S.C. Gallo, H. Dong, Vacuum **84** (2), 321-325 (2010).
[19] K. Malkiewicz, M. Sztogryn, M. Mikulewicz, A. Wielgus, J. Kaminski, T. Wierzchon, Arch. Civ. Mech. Eng. **18** (3), 941-947 (2018).
[20] M.E. Orazem, B. Tribollet, Electrochemical impedance spectroscopy, Wiley, New Jersey-Hoboken (2008).
[21] D. Grygier, V. Hoppe, A. Ziety, M. Rutkowska-Gorczyca, Eng. Biomater. **146,** 8-13 (2018).
[22] Y. Sun, X.Y. Li, T. Bell, J. Mater. Sci. **34** (19), 4793-4802 (1999).
[23] T. Wierzchon, E. Czarnowska, J. Morgiel, A. Sowinska, M. Tarnowski, A. Rogulska, Arch. Metall. Mater. **60** (3B), 2153-2159 (2015).
[24] T. Borowski, J. Jelenkowski, M. Psoda, T. Wierzchon, Surf. Coat. Techn. **204** (9), 1375-1379 (2010).
[25] Y.S. Al Jabbari, J. Fehrman, A.C. Barnes, A.M. Zapf, S. Zinelis, D.W. Berzis, Coatings, **2** (3), 160-178 (2012).
[26] A. Wichelhaus, M. Geserick, R. Hibst, F.G. Sander, Dental Materials, **21** (10), 938-945 (2005).